Experimental Study on the Failure Pattern of Cohesive Soil Under Finned Slabs Through Load Testing

Megasim[1], M. Yusuf[1*], Vivi Bachtiar[1]
Tanjungpura University, Pontianak, Indonesia[1]
*E-mail address: m_yusuf@civil.untan.ac.id

ABSTRACT

Rapid infrastructure development requires reliable pavement systems, particularly on cohesive soils with low bearing capacity. This research investigates the addition of fins to pavement slabs as an innovative rigid pavement design. The study investigates how fins and their varying inclination angles (0°, 30°, 60°, 90°) affect soil failure patterns, load bearing capacity, and deformation. Experimental tests were performed using a direct loading method with a jack on slab specimens placed in an acrylic box filled with cohesive soil. The results showed variations in soil failure patterns. The finless slab and 90° fin slab experienced shallow local shear failure, while the 0° fin slab exhibited punching shear failure due to stress concentration and vertical penetration. In contrast, the 30° and 60° finned slabs developed broader plastic zones resembling general shear failure, indicating improved stress distribution. Performance results showed the 60° finned slab achieved the highest ultimate load of 10.60 kN with the smallest settlement of 10.59 mm. The 30° fin slab carried 6.20 kN with settlement of 22.02 mm, the 90° fin slab 4.00 kN with 29.88 mm, and the 0° fin slab 3.53 kN with 50 mm, slightly better than the unfinned slab at 3.40 kN with 50 mm. The implications suggest that adding fins, particularly at 60°, can significantly enhance bearing capacity, reduce soil deformation, and restrain horizontal soil movement, making it a promising solution for pavements on soft cohesive soils.

Keywords: bearing capacity, cohesive soil, failure pattern, finned slab, rigid pavement

1. INTRODUCTION

Pavement structure is one of the key elements in road infrastructure that plays a crucial role in supporting smooth transportation, which ultimately contributes to economic growth.[1] In areas with soft soil and peat conditions, such as those commonly found in Pontianak City, the extremely low soil bearing capacity poses a major challenge in road infrastructure development.[2] Pontianak City has been actively constructing roads using rigid pavement (concrete roads) to replace flexible pavement (asphalt roads). However, despite the high initial costs of constructing concrete roads, damage still occurs relatively quickly.[3] Some sections of the road have experienced cracking, wear, and even tilting, indicating that the construction model or design applied is still not optimal.[4]

In Pontianak City, the widespread distribution of peat and soft soil makes reinforced concrete road construction with retaining walls on the road shoulders a commonly used method (Figure 1). [5] The inability of pavement structures to withstand significant lateral pressure due to horizontal movement of soft soil beneath the slab, especially in cohesive soils, can cause instability and differential settlement of the road pavement.[6]

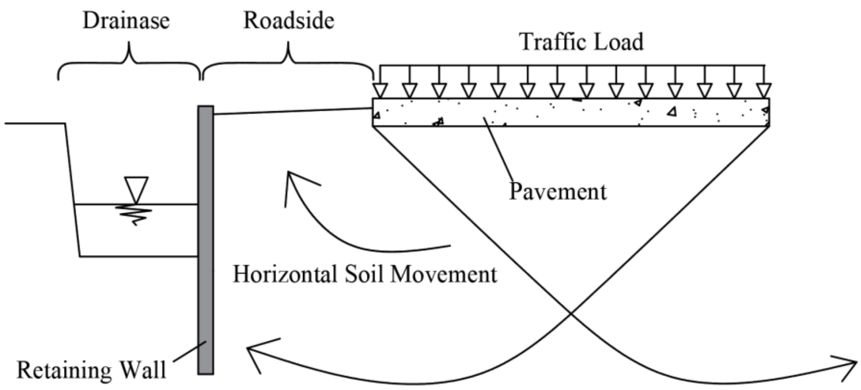

Figure 1. Horizontal subgrade movement under the slab caused by traffic loading

One innovation to enhance pavement load bearing capacity is by adding fin elements to the sides of concrete slabs. Previous studies have shown that adding fins can significantly increase the ultimate load (P_u) by 42% compared to unfinned slabs on soft soils.[6] Based on these considerations, this research presents an experimental study on the failure pattern of cohesive soil under finned slabs through load testing, aiming to observe and compare failure patterns and deformation in cohesive soils beneath unfinned slabs and finned slabs with varying fin inclinations (0°, 30°, 60°, and 90°). Load tests were conducted using slab models sized 14 cm × 14 cm with 7 cm long, 0.5 cm thick fins (Figure 2). The P_u of each slab was measured to determine the most effective fin inclination for improving soil bearing capacity.

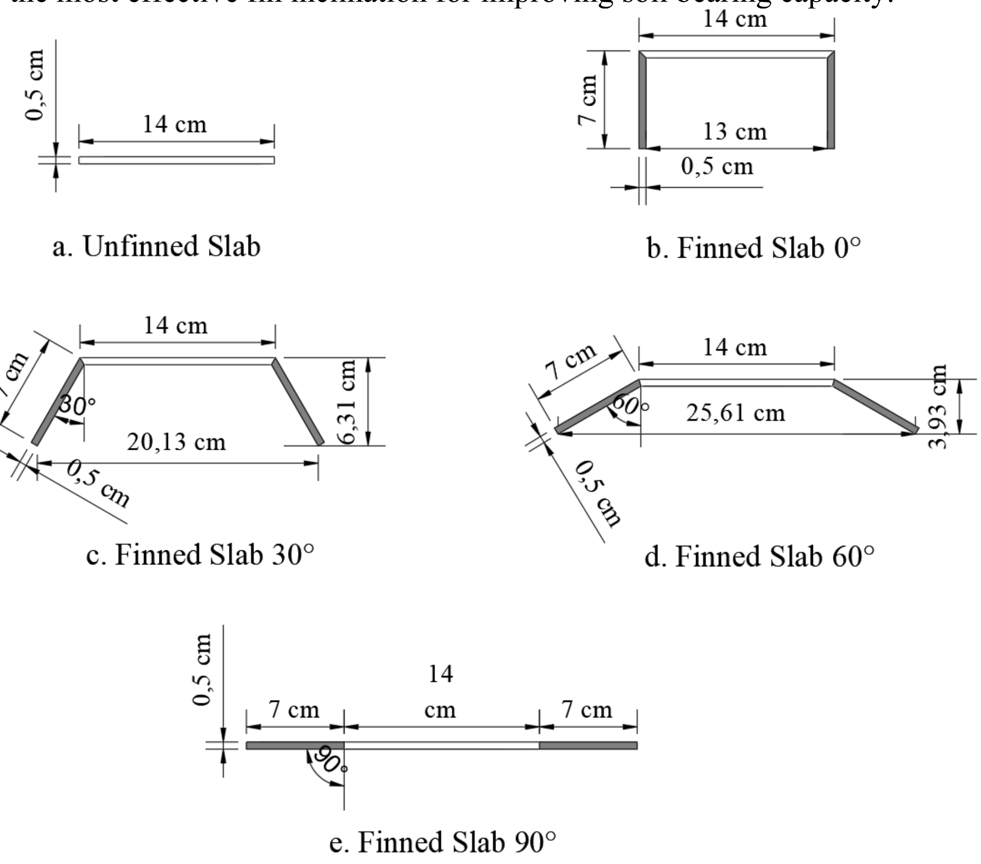

Figure 2. Front view of the slab model

2. THEORY AND METHODS

2.1 Theory

Previous Research

Several previous studies have investigated the behavior of concrete slabs on soft soils. The findings indicate that adding fins to concrete slabs can significantly increase P_u by 42% compared to unfinned slabs on soft soils.[7] Further research involving inclined fins at angles of 0°, 10°, 20°, 30°, and 40° demonstrated that a 30° angle is the most efficient configuration for minimizing settlement and improving soil bearing capacity.[8] In addition, the longer the fins added to the slab, the greater the improvement in soil bearing capacity.[9]

Cohesive Soils

Cohesive soil is a fine grained soil, such as clay, characterized by high interparticle cohesion and shear strength that depends on its internal cohesion.[10] This type of soil has low permeability, high plasticity, and is highly susceptible to volume changes due to variations in moisture content.[11] Cohesive soil is also prone to consolidation and plastic deformation under loading, making it a common challenge in construction, particularly in road infrastructure development.[12]

Terzaghi's Bearing Capacity Theory

Terzaghi's Terzaghi's classical bearing capacity theory provides the analytical basis for evaluating the ultimate load a shallow foundation or slab can support without failure.[13] The general form for a strip footing is:

$$q_u = cN_c + D\gamma Nq_q + 0{,}5\gamma BN_\gamma \quad (1)$$

Where,

q_u = ultimate bearing capacity
c = cohesion
q = overburden pressure
γ = unit weight of soil
B = footing width
$Nc, Nq, N\gamma$ = bearing capacity factors, depending on internal friction angle (φ)

Failure Pattern

In geotechnical engineering, Terzaghi classifies foundation failure patterns into general shear failure, local shear failure, and punching shear failure.[14] These patterns describe how the soil beneath a foundation deforms and fails under loading, and they play a critical role in evaluating the bearing capacity and deformation behavior of foundations.[15]

Metode Elastis Plastis

The elastic plastic method is used to analyze soil behavior from the elastic to plastic state when the applied load exceeds the elastic limit. This model provides a more realistic prediction of soil deformation and failure. The ultimate load (P_u) is determined from the intersection point of the elastic and plastic lines on the load deformation graph.[16] The graph is generated and analyzed using the Curve Expert software.

2.2 Methods

The research flow is shown in Figure 3. The experimental study tested slab models (14 × 14 cm), both unfinned and finned, with fins 7 cm long and 0.5 cm thick at inclinations of 0°, 30°, 60°, and 90°. Soil parameters (water content, unit weight, cohesion, and friction angle) were obtained from laboratory tests on the same cohesive soil used in the experiments. A preliminary test was first conducted to ensure the design feasibility. The test box measured 97 × 16 × 40 cm, adapted to the beam flexural strength testing machine. Based on Terzaghi's bearing capacity theory, the maximum assumed load was 15 kN, at which failure was expected to reach the box sides. Initially, all sides were made of 0.5 cm glass, but the front and back walls were replaced with 0.5 cm acrylic after they failed to withstand the jack load. Steel slabs were used instead of thin concrete due to dimensional limitations. To visualize soil failure, each 3 cm soil layer was covered with ±1 cm flour until reaching 35 cm in height. The arrangement of components and dial gauges is shown in Figures 4 and 5. The slab was embedded beneath the jack load, and loading was applied gradually until failure, defined as settlement beyond dial gauge capacity or 5 cm.

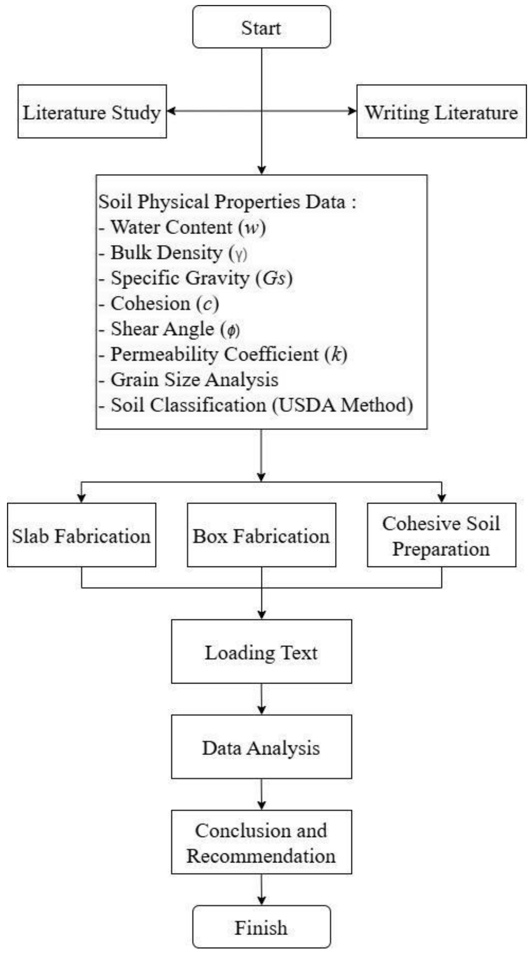

Figure 3. Flowchart of the research methodology

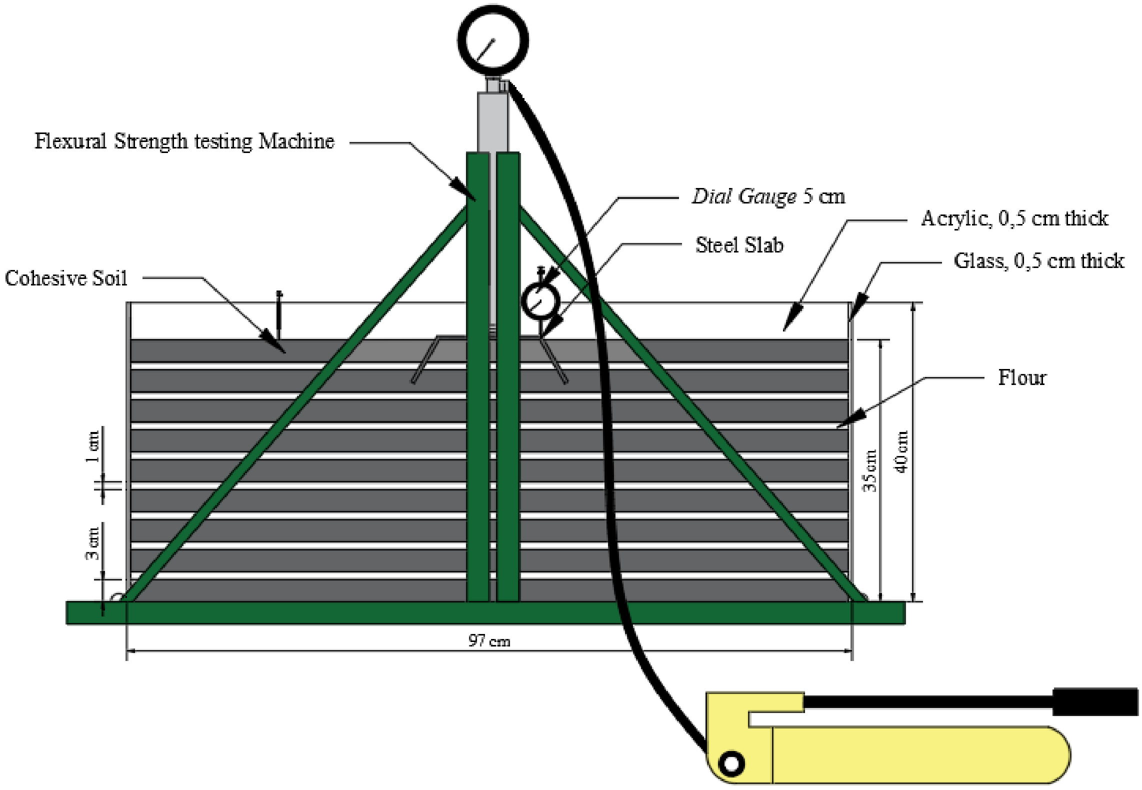

Figure 4. Front view of experimental tests model of soil failure pattern

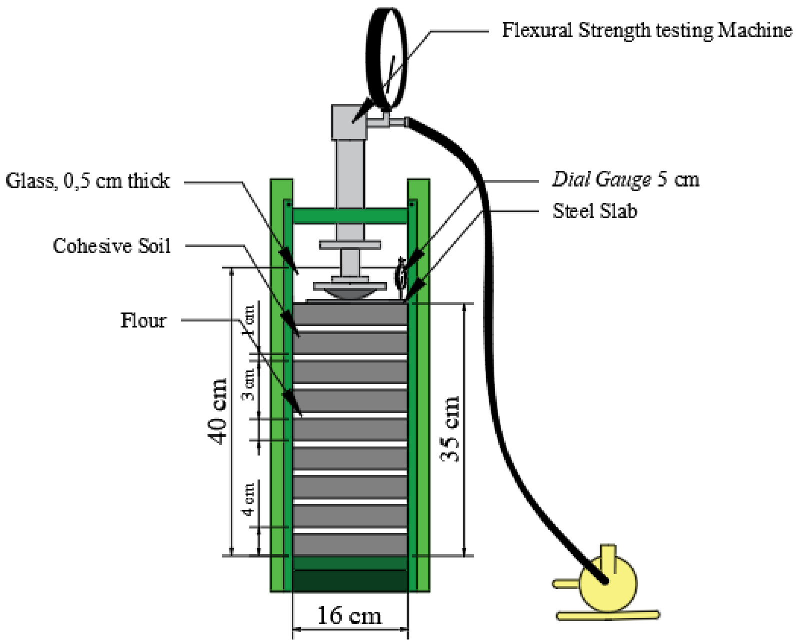

Figure 5. Side view of experimental tests model of soil failure pattern

Figure 6. Front view of experimental tests of soil failure pattern

Figure 7. View of the slab under load

3. RESULTS AND DISCUSSION

Soil Physical Properties Data

Laboratory test results on soil physical properties are presented in Table 1, based on data from Soil Mechanics Laboratory

Table 1. Soil Properties Based on Laboratory Tests

Soil Parameters	Unit	Data
Soil Type	-	Silty Clay Loam
Water Content (*w*)	%	113.450
Bulk Density (γ)	kN/m³	13.930
Specific Gravity (*Gs*)	-	2.693
Cohesion (*c*)	kPa	3.530
Shear Angle (*ϕ*)	°	16.666
Permeability Coefficient (*k*)	m/s	7.44×10^{-7}

Analysis of Soil Failure Patterns

In this study, slab loading tests were conducted on cohesive soils to investigate the soil failure patterns under vertical loads and determine the influence of fin inclination on bearing capacity and soil deformation behavior.

1. The test on the unfinned slab showed a local shear failure with partial soil displacement and no significant heaving. At a 9 kN load, the soil settled 50 mm. Stress was concentrated near the edges, with limited penetration and interaction. This resulted in low bearing capacity and rapid settlement, indicating the slab is unsuitable for soft cohesive soils without improvement.

Figure 8. Failure pattern of cohesive soil under the unfinned slab sample

2. The finned slab with 0° inclination was tested, it also failed at 9 kN under similar settlement conditions. However, unlike the unfinned slab, the vertical fins acted as passive resistors to downward movement but did not effectively spread the load laterally. The soil exhibited a punching shear failure, marked by vertical penetration without significant lateral deformation or heaving. This suggests that at 0° inclination, the fins had minimal contribution in enhancing the soil's shear resistance or redistributing stress.

Figure 9. Failure pattern of cohesive soil under the finned slab sample with 0° inclination

3. The finned slab with 30° inclination showed improved performance compared to the previous two. Failure occurred at a higher load of 15 kN, and local shear failure was observed. At 10 kN, slight ground heaving was detected, indicating that the inclined fins began to redirect part of the vertical load laterally into the soil. This redirection helped initiate a wider shear zone, although it was still not fully developed. The 30° fins increased interaction between the slab and the soil mass, showing better stress redistribution, although still not as optimal as steeper inclinations.

Figure 10. Failure pattern of cohesive soil under the finned slab sample with 30° inclination

4. The finned slab with 60° inclination. This slab endured the highest load of 20 kN before failure, with local shear failure becoming visible after 8 kN. Ground heaving began at around 13 kN, suggesting a substantial lateral pressure buildup beneath the slab. The 60° fins effectively redirected vertical forces outward, resulting in a broader shear zone and improved stability. Although the failure was not yet general shear failure, the pattern indicated a transition toward it, reflecting enhanced stress dispersion and deeper load influence in the soil.

Figure 11. Failure pattern of cohesive soil under the finned slab sample with 60° inclination

5. The finned slab with 90° inclination exhibited local shear failure at 12 kN. Ground heaving was observed early at around 5 kN, yet the failure pattern remained limited in scale. The vertical fins partially redirected stress laterally but restricted deeper soil engagement due to their upright geometry.

Figure 12. Failure pattern of cohesive soil under the finned slab sample with 90° inclination

Analysis of Soil Deformation

This section summarizes the soil deformation results from slab loading tests, with load-settlement data were analyzed using CurveExpert to determine deformation behavior, curve models, and P_u.

Table 2. Deformation Results of Settlement for All Slab Sample Variations

P **(kN)**	***d*** **(mm)**				
	Unfinned Slab	**Finned Slab 0°**	**Finned Slab 30°**	**Finned Slab 60°**	**Finned Slab 90°**
0	0.000	0.000	0.000	0.000	0.000
1	0.218	0.207	0.243	0.768	0.200
2	1.425	0.808	0.720	1.616	1.901
3	4.326	4.297	2.403	2.575	4.553
4	13.433	17.968	4.157	3.626	8.685
5	24.847	30.406	6.216	4.686	11.307
6	32.004	36.211	9.613	5.706	15.199
7	37.448	40.587	13.648	7.201	20.832
8	42.873	43.761	17.948	8.847	26.216
9	50.000	50.000	22.024	10.594	29.878
10			26.252	12.301	36.302
11			31.545	13.836	41.245
12			36.818	15.573	50.000
13			41.929	17.774	
14			45.832	18.865	
15			50.000	21.117	
16				24.924	
17				27.439	
18				31.428	
19				44.042	
20				50.000	

The loading test on the unfinned slab showed a maximum settlement of 50 mm under a peak load of 9 kN. The curve remained linear up to 1.425 mm before softening, with the Hoerl model estimating an P_u of 3.40 kN at 0.43 mm. The 0° finned slab also reached 9 kN, with linear behavior up to 0.808 mm; the P_u was 3.53 kN. The 30° finned slab withstood 15 kN with P_u of 6.20 kN at 2.30 mm, maintaining linearity up to 4.157 mm. The 60° finned slab reached a peak load of 20 kN, with linear behavior up to 8.847 mm and a $P_u$of 10.60 kN. Meanwhile, the 90° finned slab carried a maximum load of 12 kN, linear up to 8.685 mm, with a P_u of 4.00 kN at 2 mm.

These results indicate that the addition of fins to the slab generally increases the P_u compared to the unfinned slab. Among all variations, the 60° inclined fin configuration produced the highest P_u, making it the most effective design for enhancing soil bearing capacity. These trends can be observed in the load settlement curves shown in Figures 13 to 17.

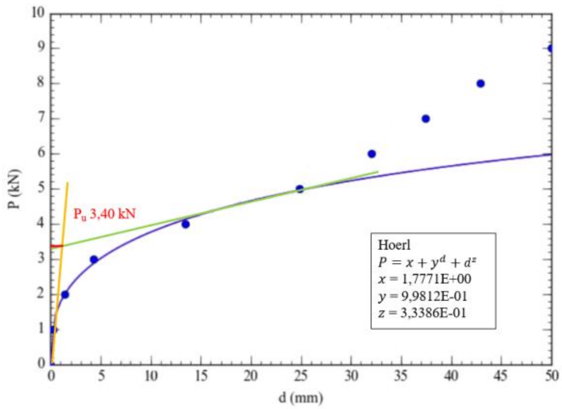

Figure 13. Graph of loading test on unfinned slab

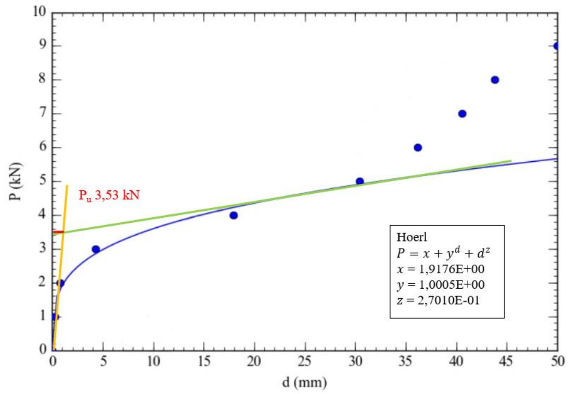

Figure 14. Graph of loading test on finned slab with 0° inclination

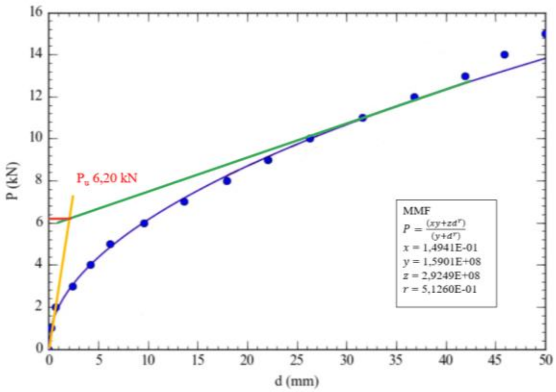

Figure 15. Graph of loading test on finned slab with 30° inclination

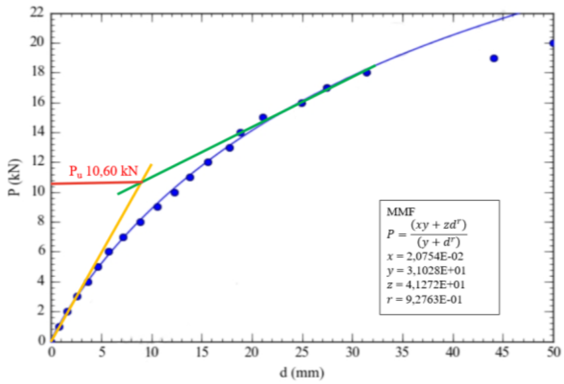

Figure 16. Graph of loading test on finned slab with 60° inclination

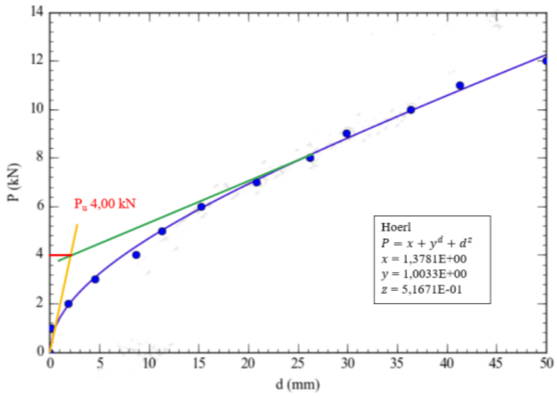

Figure 17. Graph of loading test on finned slab with 90° inclination

4. CONCLUSIONS

Based on the analysis, the failure patterns and stress distribution varied with fin inclination. Slabs without fins and those with 90° fins showed local shear failure and shallow plastic zones. A 0° fin caused vertical stress concentration and punching shear, while 30° and 60° fins directed stress diagonally, enlarging the shear zone and improving load distribution.

The P_u was also influenced by fin angle. The slab without fins had a P_u of 3.40 kN, increasing slightly to 3.53 kN at 0°, then rising significantly to 6.20 kN at 30°, and peaking at 10.60 kN at 60°. It dropped to 4.00 kN at 90°, showing that 60° offered the best performance.

In conclusion, the 60° finned slab provided the most favorable failure pattern, widest plastic zone, highest bearing capacity, and lowest settlement, as shown by its stable load-deformation curve. This study was limited to laboratory scale with a fixed fin geometry; thus, further research is needed before applying the findings to full-scale pavement.

REFERENCES

[1] M. Zhao, Y. Liu, C. Wu, X. Xu, Y. Pei, and C. Zhang, "Pavement bearing capacity evaluation during pavement-fracturing using falling-weight impact acceleration," *Case Stud. Constr. Mater.*, vol. 21, Dec. 2024, doi: 10.1016/j.cscm.2024.e04002.

[2] M. Yusuf, V. Bachtiar, and S. Mayuni, "UJI KEKUATAN PELAT BETON BERSIRIP DI ATAS TANAH GAMBUT BERLAPIS PASIR SETINGGI SETENGAH SIRIP," in *Prosiding Seminar Nasional Penerapan Ilmu Pengetahuan dan Teknologi 2015*, Z. Panjaitan, Seno D.; Bariyah, Nurul; Zain, Ed., Pontianak: Badan Penerbit Universitas Tanjungpura (UNTAN Press), 2015, pp. 93–98.

[3] W. R. Azzam and A. Basha, "Utilization of soil nailing technique to increase shear strength of cohesive soil and reduce settlement," *J. Rock Mech. Geotech. Eng.*, vol. 9, no. 6, pp. 1104–1111, 2017, doi: 10.1016/j.jrmge.2017.05.009.

[4] V. Bachtiar and M. Yusuf, "UJI KEKUATAN PELAT BETON BERSIRIP YANG DIPERKAKU DENGAN CARA PENEBALAN DI DAERAH SAMBUNGAN ANTARA PELAT DAN SIRIP," in *Prosiding Seminar Nasional Penerapan Ilmu Pengetahuan dan Teknologi 2016*, D. Zain, Zairin; Bariyah, Nurul; Astiani, Ed., Pontianak: Badan Penerbit Universitas Tanjungpura (UNTAN Press), 2016, pp. 357–362.

[5] V. Candra; Yusuf, M; Bachtiar, "TINJAUAN DAYA DUKUNG PELAT BETON BERSIRIP DI ATAS TANAH GAMBUT DENGAN VARIASI KETEBALAN LAPISAN PASIR," *JeLAST J. Tek. Kelaut. , PWK , Sipil, dan Tambang*, vol. 5, no. 1, 2018, [Online]. Available: https://jurnal.untan.ac.id/index.php/JMHMS/article/view/24026/18825

[6] J. Bauer, H.-G. Kempfert, and O. Reul, "Lateral pressure on piles due to horizontal soil movement," *Int. J. Phys. Model. Geotech.*, vol. 16, no. 4, pp. 173–184, Jan. 2016, doi: 10.1680/jphmg.15.00005.

[7] M. Setiawan, M. Yusuf, and V. Bachtiar, "Uji Kekuatan Pelat Bersirip Yang Diperkaku Dengan Cara Penebalan Di Daerah Sambungan Antara Pelat Dan Sirip (Studi Kasus: Penebalan Pada Pelat)," *JeLAST J. PWK, Laut, Sipil, Tambang*, vol. 5, no. 1, pp. 1–11, 2018, [Online]. Available: https://jurnal.untan.ac.id/index.php/JMHMS/article/view/23915

[8] S. M. Sirait, V. Bachtiar, and M. Yusuf, "TINJAUAN DAYA DUKUNG PELAT BETON BERSIRIP DI ATAS TANAH LEMPUNG DENGAN VARIASI KEMIRINGAN SIRIP BERDASARKAN UJI PEMBEBANAN," *JeLAST J. PWK, Laut, Sipil, Tambang*, vol. 9, no. 2, pp. 1–9, 2022, [Online]. Available: https://jurnal.untan.ac.id/index.php/JMHMS/article/view/55267/75676593584

[9] T. I. Amal, V. Bachtiar, and M. Yusuf, "Review Of Bearing Capacity Of Finned Concrete Slabs Based On The Numerical Variation Of Length," *J. Tek. Sipil*, vol. 23, no. 3, pp. 438–445, Aug. 2023, doi: 10.26418/jts.v23i3.6.

[10] Z. Nosrati and S. M. Binesh, "Mesh-free kinematic shakedown analysis of cohesive soils," *Int. J. Geo-Engineering*, vol. 15, no. 1, pp. 1–24, 2024, doi: 10.1186/s40703-024-00209-1.

[11] A. Van Lerberghe, K. S. O. Li, A. D. Barr, and S. D. Clarke, "High strain rate behaviour of cohesive soils," *Int. J. Impact Eng.*, vol. 198, no. November 2024, p. 105189, 2025, doi: 10.1016/j.ijimpeng.2024.105189.

[12] K. A. A. Wicaksana, Z. Zakaria, D. Muslim, and N. Khoirullah, "Soil Bearing Capacity of Shallow Foundation Based on Terzaghi Method in Cipatat, West Bandung, West Java," *J. Geol. Sci. Appl. Geol.*, vol. 4, no. 1, pp. 17–22, 2020, [Online]. Available: http://jurnal.unpad.ac.id/gsag/article/view/28998

[13] M. Aytekin, "Estimating bearing capacity of shallow foundations by artificial neural networks," *Chall. J. Struct. Mech.*, vol. 3, no. 4, p. 151, 2017, doi: 10.20528/cjsmec.2017.11.016.

[14] Isnaniati and I. B. Mochtar, "Increasing the Bearing Capacity of Shallow Foundations on Soft Soil After the Installation of Micro-Piles," *J. Civ. Eng. Forum*, vol. 9, no. September, pp. 227–238, 2023, doi: 10.22146/jcef.5925.

[15] M. xiang Peng and H. xi Peng, "The ultimate bearing capacity of shallow strip footings using slip-line method," *Soils Found.*, vol. 59, no. 3, pp. 601–616, 2019, doi: 10.1016/j.sandf.2019.01.008.

[16] A. J. Zedan, "Pressure - Settlement Characteristics of Shallow Foundations using Finite Element Method," *Tikrit J. Eng. Sci.*, vol. 24, no. 1, pp. 25–37, 2017, doi: https://doi.org/10.25130/tjes.24.1.03.